# Failure of fluorocarbon copolymer pipes subjected to mechanical strain in an alkaline environment

Luca Cozzarini [a,*], Chiara Schmid [a]

[a] Department of Engineering and Architecture, University of Trieste, Via Valerio 6A, I-34127 Trieste, Italy

ARTICLE INFO

*Keywords:*
Fluorocarbon polymers
Stress corrosion cracking
Alkaline solution
Mechanochemical degradation
Dehydrofluorination

ABSTRACT

A failure analysis was carried out on leaking fluorocarbon-based copolymer pipes used in a cleaning and disinfection plant. Pipes conveyed a solution of sodium hydroxide and showed leaking after two months of service. Leaks originated from reddish-colored cuts located on the bending curves of the external surface of the pipes. Experimental findings and literature review pointed out that a combined effect of chemical degradation and mechanical strain (similar to stress corrosion cracking) triggered the failure. This type of degradation developed in high pH hydroxide solution due to dehydrofluorination of the exposed surface, starting material embrittlement and formation of crazes and microcracks. An applied mechanical deformation accelerated the crack opening and the solvent diffusion, up to the consequent pipe leaking and failure.

## 1. Introduction

Poly (vinylidene fluoride) (PVDF) is a high molecular weight semi-crystalline polymer obtained from the polymerization of 1,1-difluoroethylene ($CH_2 = CF_2$). It is widely used in engineering applications such as piping, gasket, filtering membranes thanks to its high mechanical, thermal and chemical stability [1–3]. Processing parameters can affect the PVDF final properties, including dielectric and mechanical properties. Depending on the crystallization conditions, PVDF may present four different polymorphs that are defined by the conformation of the polymer chains and their crystalline structure: the orthorhombic α, β and δ phases and the monoclinic γ phase [4–6]. PVDF is rigid, and it is generally poorly suited for objects subject to bending like pipes. It can be co-polymerized to obtain a flexible material such as the poly[vinyl fluoride]-co-[hexafluoropropylene] [PVDF-co-HFP] [7]. PVDF and its copolymers are able to resist several chemicals and harsh conditions; nevertheless, the detrimental effects of strong hydroxide solutions are well known [3,8,9]. This copolymer used to manufacture the flexible pipes studied in this work is known under the trade name Arkema Kynarflex® 2800. According to the manufacturer's datasheet [10,11], this material is able to withstand several chemicals and harsh conditions. Concerning the reported case, it can resist an aqueous sodium hydroxide [NaOH] solution with a concentration of up to 10% wt. [pH $\leq$ 13.5] at a maximum temperature of 50 °C; it is not recommended for use at room temperature with NaOH solution with a concentration greater than 50% wt. Several cases of environmental stress cracking affecting PVDF products in service are reported [9,12–14] few of them concern also its copolymers and similar fluorocarbon polymers [15,16]. In order to improve the stability of this specific material in service conditions, it is essential to analyze the failure and understand if the same degradation mechanism applies also on this particular copolymer.

* Corresponding author.
*E-mail address:* lcozzarini@units.it (L. Cozzarini).

Accepted 23 June 2021

## 2. Material and methods

### 2.1. Background and failure description

Pipes [outer diameter 12 mm, inner diameter 10 mm] made in Arkema Kynarflex® 2800 fluorinated copolymer were used to convey NaOH aqueous solution in an industrial disinfection/cleaning plant located in northern Italy. According to the plant management, NaOH solution had a concentration of 30% wt., and the plant operated at room temperature [15–35 °C]. According to plant schematics, pipes were bent with a radius between 90 and 130 mm. It is worth pointing out that, even if regarded as "flexible" with respect to the PVDF homopolymer, Kynarflex® 2800 has a limiting bending radius which is a function of pipe diameter [10]. For the pipes of the examined case [outer diameter 12 mm], the minimum recommended bending radius is 85 mm. Pipes showed multiple leaking points next to the external surface of bending curves, after two or three months of service. The leaking points were characterized by well visible cuts with reddish edges and surfaces. The cut lines were perpendicular with respect to the pipe axis [circumferential cracks].

### 2.2. Materials and methods

Samples of Kynarflex® 2800 were received from failed sections of the pipes. New [unused] sections were used as control samples. Selected sections were cut off with scissors for further analysis. Samples were analyzed via visual examination, optical microscopy [OM], scanning electron microscopy [SEM], Fourier Transform Infrared spectroscopy [FT-IR] and Differential Scanning Calorimetry [DSC]. OM images were acquired by an Optika SZN-2 stereo microscope. SEM investigation was performed by a Leica Stereoscan 430i equipped with a Pentafet Plus TM detector for Energy Dispersive Spectrometry [EDS] analysis. FT-IR spectra were acquired via a Thermo-Nicolet Nexus 470 spectrometer, equipped with an Attenuated Total Reflectance [ATR] accessory. Differential Scanning Calorimetry [DSC] measures were carried out by means of a Netzsch DSC 200 F3 Maia in nitrogen atmosphere, at a heating rate of 10 K/min.

### 2.3. Methodology

First, failure background, operating condition, available technical datasheets and chemical resistance charts were thoroughly examined to determine the events chain that led to the failure. Then, failed samples were compared to new ones [control samples] with different techniques. Visual examination was performed to assess the location and the macroscopic appearance of failures; optical and electron microscopy to investigate the morphological details of the cuts; EDX and FT-IR to characterize the chemistry of the degradation mechanism, in particular on reddish areas close to the cuts. DSC was performed to assess possible alteration in the sample crystallinity due to degradation. Moreover, to simulate and monitor the degradation mechanism in an alkaline environment, specimens taken from control samples were immersed in NaOH solution [30% and 60% wt.] and their FT-IR spectra monitored over time [from 6 to 42 days].

## 3. Results and discussion

### 3.1. Visual examination and optical microscopy

Evident cuts in the location of the leaking points are visible Fig. 1. These cuts are located on the pipe bends and pass through the entire wall thickness. The surface of the cuts is red-colored; in many cases, reddish stains can also be noticed in the internal surface of

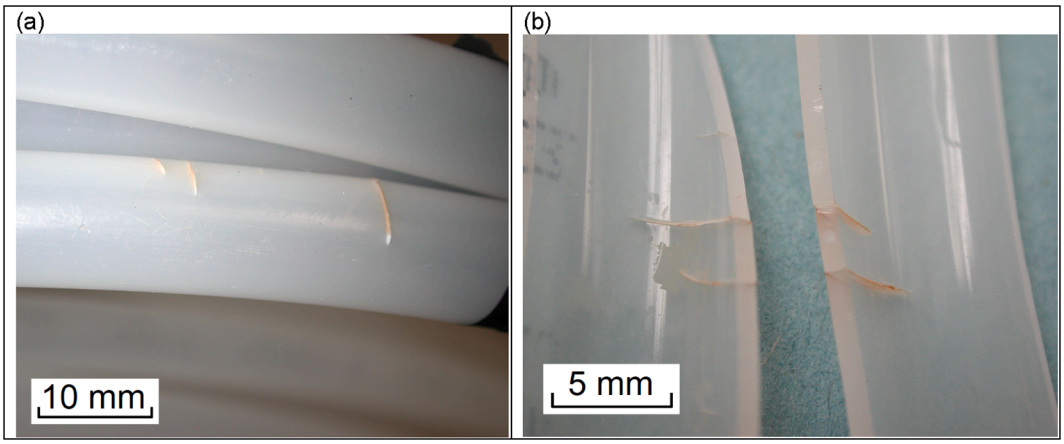


**Fig. 1.** Cuts on the pipe surface: (a) external view and (b) internal and section view.

the pipe Fig. 2. Details of two different cuts, as seen at OM examination, are shown in Fig. 3. The cut edges appear rough and jagged; a network of material partially interconnecting the opposing walls of the cut can be seen. Fig. 4a and Fig. 4b shows several rough, whitened and scratched location, as well as areas with an irregular surface on the inner wall of the pipes. The white, parallel scratches are perpendicular with respect to the pipe axis [circumferential cracks]. Samples subjected to artificial ageing in alkaline solution are shown in Fig. 5. Samples immersed in 30% wt. NaOH does not show any noticeable change in their color after 42 days. On the other hand, those immersed in 60% wt. NaOH became reddish after 28 days, and dark red after increasing immersion times.

### 3.2. *Scanning electron microscopy*

SEM images of the final part of a cut [apex, or crack edge] are shown in Fig. 6a. It is possible to notice a network of material partially interconnecting the opposing walls of the crack, as already noticed in OM images. The details of the opening edge are shown in Fig. 6b. At higher magnification [Fig. 7] indented fracture edges and discontinuous plastic deformation around the crack tip are noticeable. Fig. 8 shows a detail of the central zone of the cut, where the progressive tearing of the interconnecting material can be seen. Similar features, already seen in OM images [Fig. 3] and in other SEM images [Fig. 6], are usually observed in crazing and environmental crazing mechanisms in several polymeric materials [17–19]. Around damaged areas, crystalline deposits can be spotted. At higher magnification, these deposits appear to be octahedral crystals Fig. 9. After EDX analysis, they were identified as crystals of sodium fluoride [NaF]. SEM of samples subjected to artificial ageing did not show any appreciable difference with respect to control samples. No difference in the fluoride to carbon ratio was registered by EDX between aged and control samples.

### 3.3. *Infrared spectroscopy*

FTIR spectra of the control sample [internal and external surfaces] are shown in Fig. 10. The typical vibrational bands related to functional groups found in fluorocarbon polymers can be identified. The bands from 3026 to 2850 $cm^{-1}$ are attributed to CH and $CH_2$ stretch; bands from 1402 to 1383 $cm^{-1}$ to $CH_2$ bending; 1279 to 1067 $cm^{-1}$ to $CF_2$ stretch; 976 to 797 $cm^{-1}$ to $CH_2$ rocking and 762–613 $cm^{-1}$ to $CF_2$ bending [5,6,20,21]. Bands related to α-phase PVDF [1383, 1207, 1148, 976, 797 and 762 $cm^{-1}$] are more intense on the spectrum acquired from the internal surface, while bands related to β phase [1279 and 839 $cm^{-1}$] are more pronounced on the one acquired from the external surface. This heterogeneous crystalline structure can be ascribed to the different cooling rates of internal and external pipe surfaces after the extrusion process. The formation of different crystalline structures in PVDF and its co-polymers, as well as their IR spectral properties, are widely reported in the literature [4,21–23].

After comparing FTIR spectra acquired on control samples to those acquired on brown/reddish areas [close to the leaking cuts of failed pipes] [Fig. 11], it is possible to notice in the latter the rising of a sharp peak at 3693 $cm^{-1}$ [Na—OH stretch], a broad band centered at 3360 $cm^{-1}$ [OH stretch] [20] and another band at 1585 $cm^{-1}$. This latter band is usually attributed to $COO^-$ stretch [chain breakdown/scission] or to $COO^-/Na^+$ stretch [saponification] [24,25]. Nevertheless, in this specific case, likewise to FT-IR data reported for fluorinated polymers subjected to alkaline degradation, the rise of this band can be related to the formation of a —C═C—C—C═C—C—conjugated double bond system [6,16]. Moreover, the intensity of CH and $CH/CH_2$ vibrations [3000–2800 $cm^{-1}$] in the failed pipes spectra rises with respect to that related to $CF_2$ vibrations [1200–1050 $cm^{-1}$], pointing out a loss of $CF_2$ groups in the polymer chain [defluorination]. More in detail, the 2926 $cm^{-1}$ and 2850 $cm^{-1}$ bands [asymmetric and symmetric $CH_2$ stretch] become more intense than the 3026–2958 $cm^{-1}$ band [CH stretch]. This also points out an increase in the intensity of vibrational bands related to $CH_2$ groups alongside the polymer chain. FTIR spectra acquired on samples subjected to simulated ageing

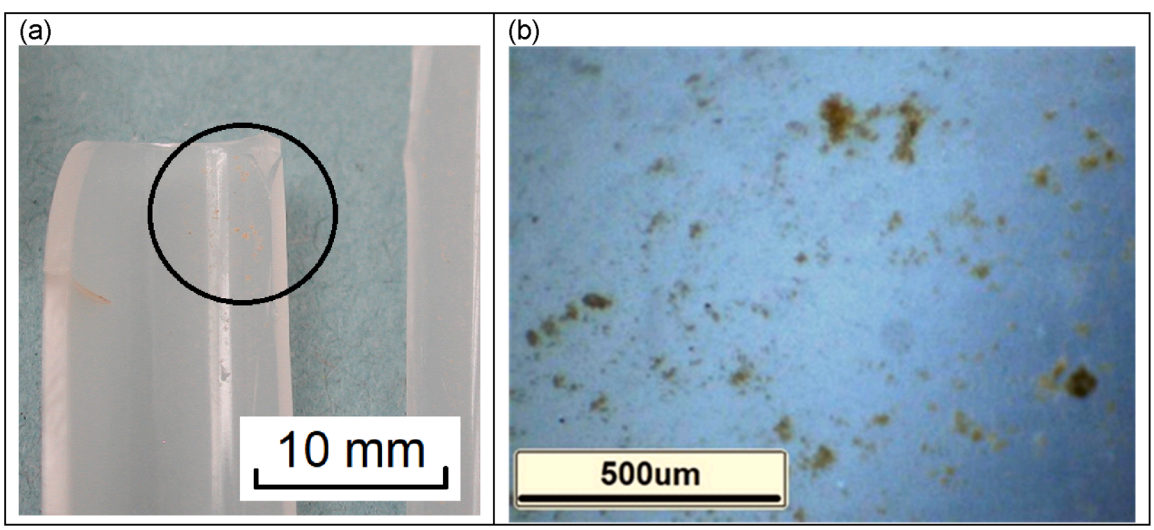


**Fig. 2.** Reddish stain seen at (a) visual examination; (b) optical microscopy.

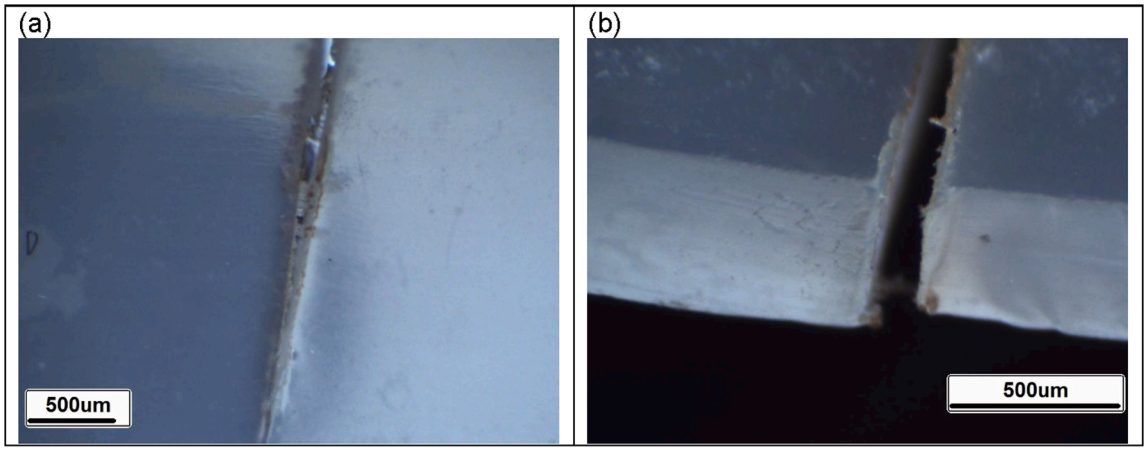


**Fig. 3.** Details of two different cuts at optical microscopy.

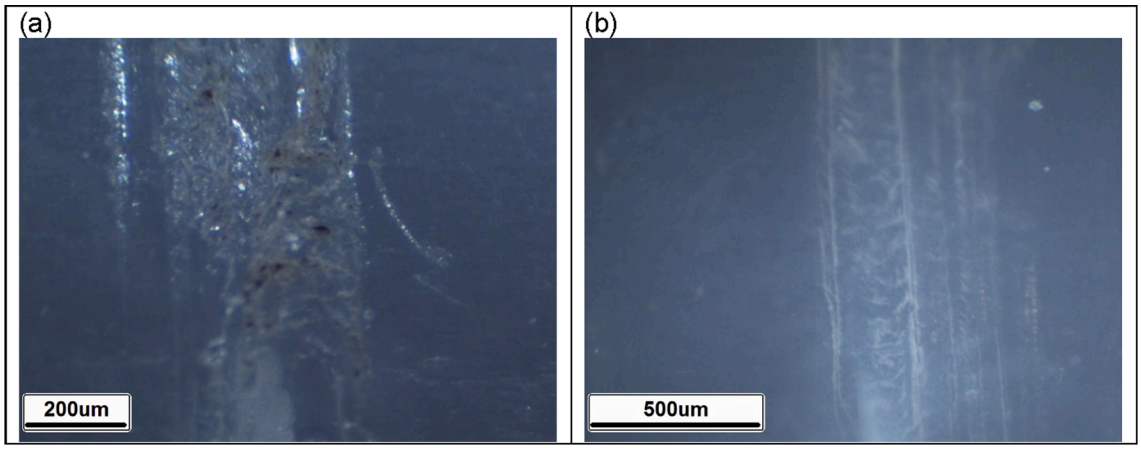


**Fig. 4.** Optical microscopy of inner pipe wall: – (a) scratched area and (b) parallel, white scratches.

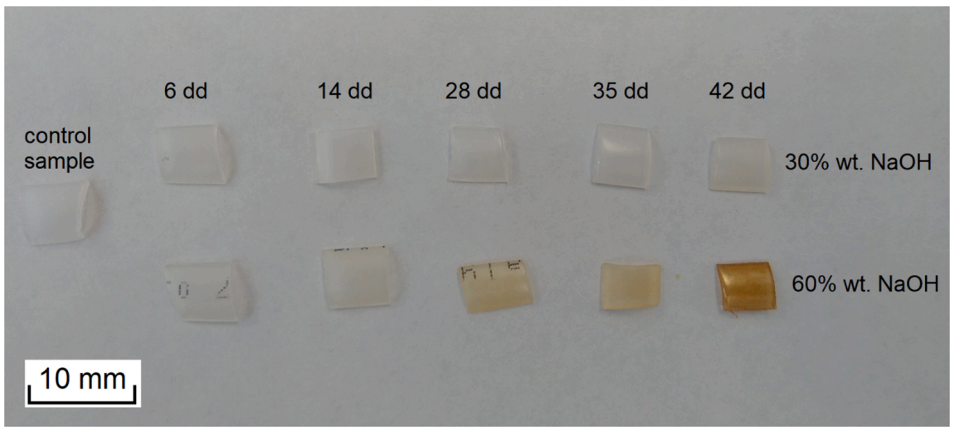


**Fig. 5.** Sample subjected to artificial ageing in: 30% wt. NaOH (upper line); 60% wt. NaOH (bottom line).

[Fig. 12 and Fig. 13] show no substantial difference for samples immersed in NaOH 30% wt. respect to control ones [even after 42 days]. No clear vibrational band related to oxidation or degradation is noticeable. On the other hand, samples immersed in NaOH 60% wt. show a clear increase in the IR band centered at 1590 $cm^{-1}$, which, as already discussed above, can be attributed to $COO^{-}/Na^{+}$

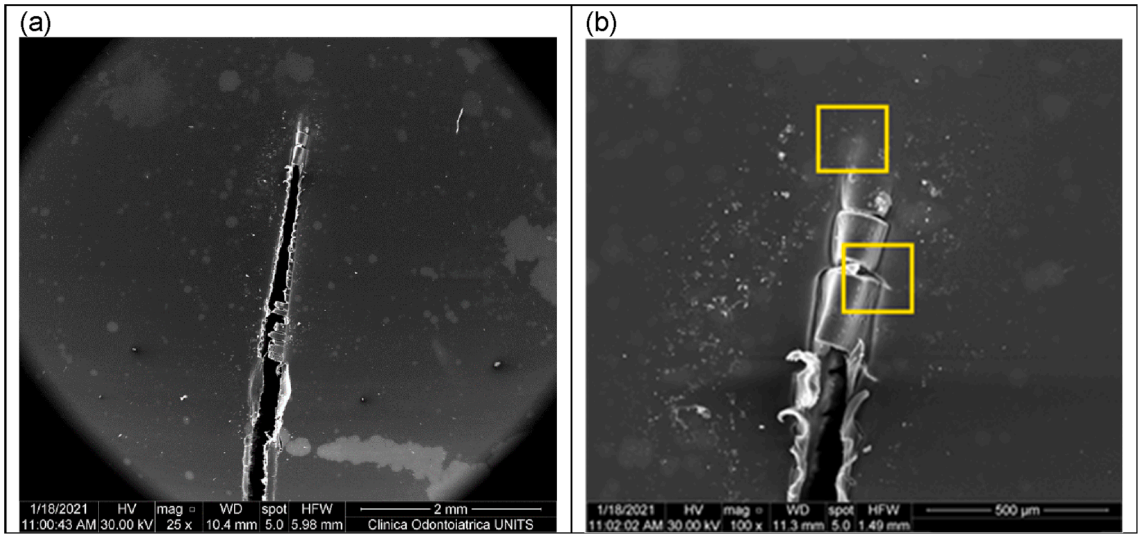


**Fig. 6.** SEM images of (a) one cut; and (b) the crack tip (apex of the cut). Highlighted areas (squares) are shown at higher magnification in Fig. 7.

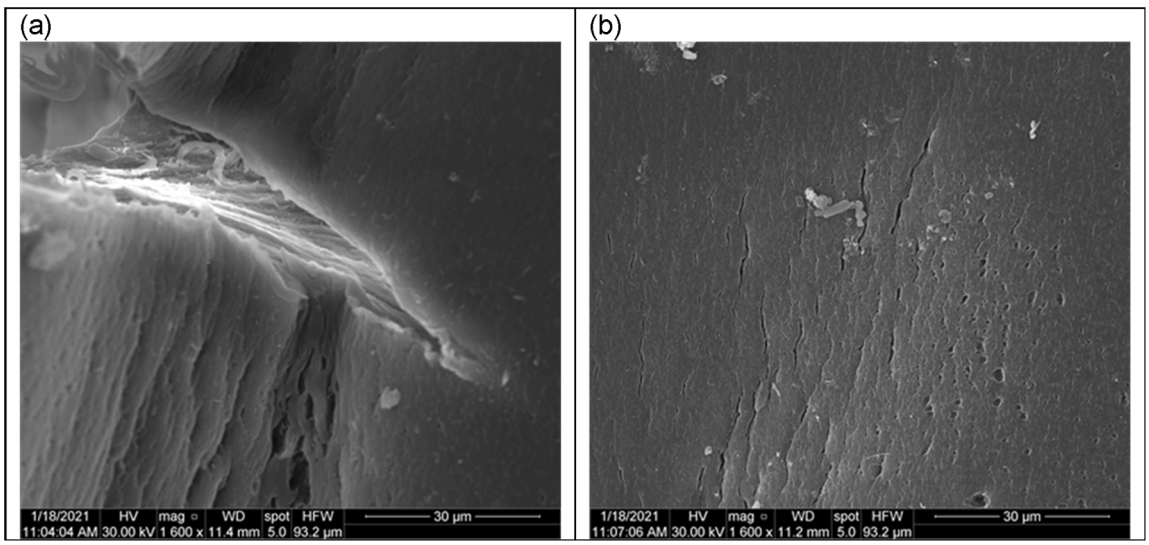


**Fig. 7.** SEM images: (a) higher magnification detail of fracture surface from Fig. 6; (b) higher magnification detail of crazes close to the crack tip from Fig. 6.

stretch [saponification] or to —C═C—C═C—C— conjugated double bond system. No change in the $CH_2/CF_2$ intensity ratio is observed in both cases, so defluorination is not apparently taking place, contrary to the behavior previously seen on the failed pipe sections spectra. This difference can be ascribed to the limited penetration depth of chemical attack in absence of an applied mechanical strain. If this depth is limited to the first layers, it could be speculated that the ATR FT-IR probes [on average] a deeper, non-degraded material volume [with diamond window, and assuming a PVDF refractive index of 1.426 [26], the instrument probing depth should be between 10 and 50 µm in the 3000–500 $cm^{-1}$ region [27]].

### *3.4. Differential Scanning Calorimetry*

Thermograms of new pipe and used pipe samples are depicted in Fig. 14. The melting peaks of new and used samples are comparable and fit well the value reported in the technical datasheet [143 °C]. The melting enthalpy of the used sample [26.2 J/g] is slightly lower than that of the control one [28.4 J/g]. No significant difference between the crystallinity of control and used samples is therefore expected. Both melting enthalpy values are about 50% with respect to the melting enthalpy reported for PVDF homopolymer [22,23,28]; it is worth remembering that this material is a commercial copolymer, and its crystallinity value is not reported.

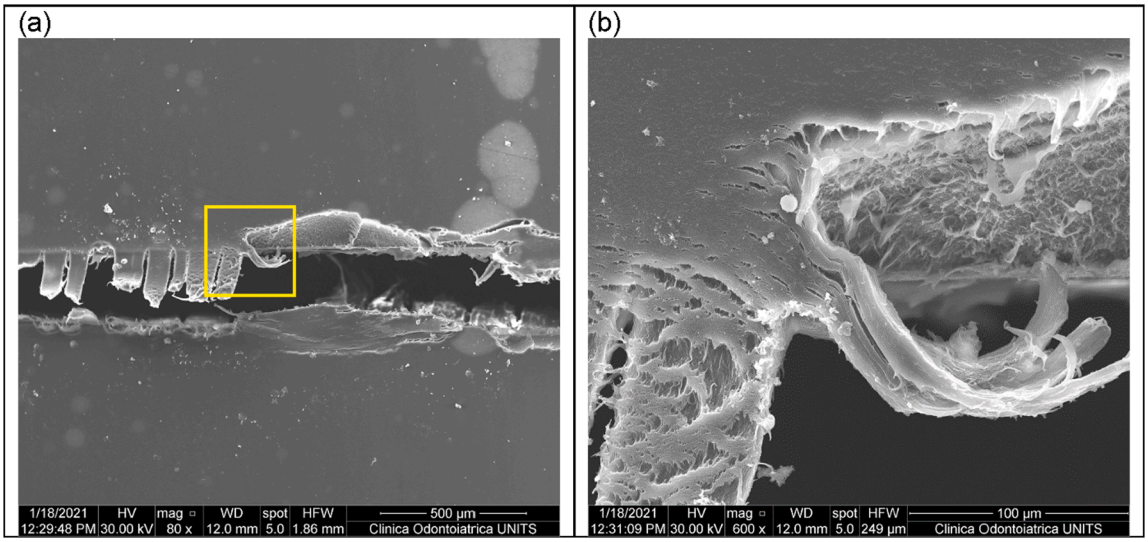


**Fig. 8.** SEM images the progressive tearing of the material interconnecting the cut surfaces. Highlighted area (square) in (a) is shown in (b).

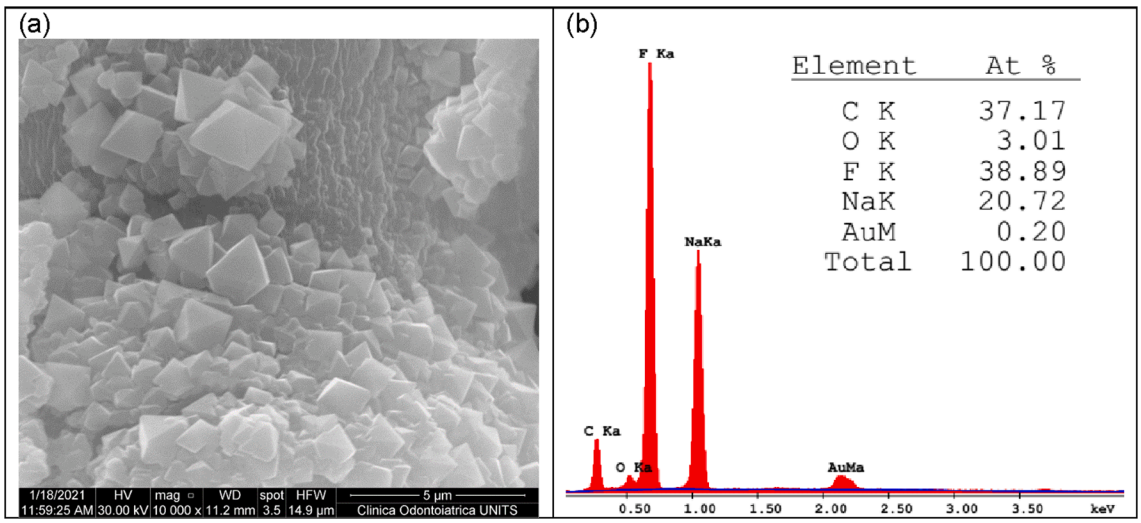


**Fig. 9.** (a) SEM images of crystalline deposits found around damaged areas; (b) EDX spectrum of crystalline deposits.

## 4. Discussion

Although PVDF is regarded as a high chemical-resistant material, its susceptibility to surface degradation in an aggressive environment [in particular alkaline solutions] is well known [3,29–31]. Most of the literature concerning practical failure cases deals with filtering membranes [9,14,29]; some cases of failed pipes are reported [32]. The most accepted degradation path of PVDF in NaOH encompasses the formation of C═C units in the polymer chain as result of the elimination of H and F [dehydrofluorination] or F [defluorination] [6,8,33,34]. The degraded surface appears reddish to brownish; sometimes, micro-cracks or crazed surfaces are observed. Failure of PVDF objects usually takes place after the combined action of alkaline environment and mechanical stress (in a manner similar to stress-corrosion cracking] [12,13,35,36]. Specifically, while the chemical attack alone is described by a diffusion-controlled process [often limited at the surface only], the simultaneous presence of an applied strain seems to accelerate the process, leading to the formation and the growth of macroscopical cracks, characterized by reddish surfaces and edges [13]. This is followed by an overall embrittlement of the degraded area and a sudden failure of the component. Most of these studies pertain to high concentrated NaOH solutions [pH greater than 13] and/or high temperatures [80–90 °C] in combination with an applied mechanical strain. Noteworthy, the work from Hinksman et al. [12] reports that, after immersing PVDF samples in 30% wt. NaOH, with applied strains below 5%, no change in color, cracking, crazing or degradation effects are noticeable. Other works show degradation effects after PVDF exposure to sodium hypochlorite (NaOCl], with degradation starting at lower concentration with respect to NaOH and even

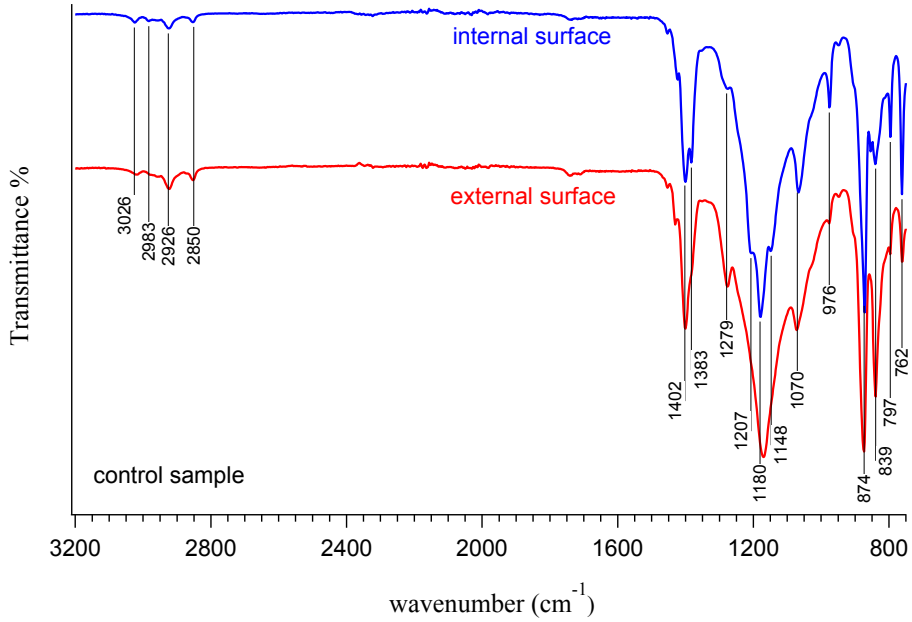


**Fig. 10.** F FTIR spectra of internal (blue curve) and external (red curve) surfaces of control samples. (For interpretation of the references to color in this figure legend, the reader is referred to the web version of this article.)

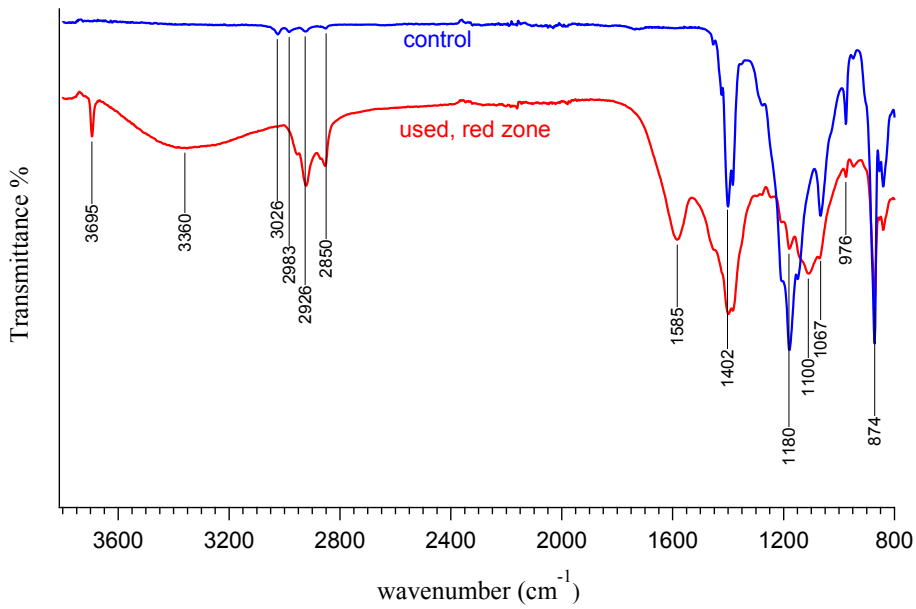


**Fig. 11.** FTIR spectra of internal surfaces of new pipe (blue curve) and brown/reddish area of used pipe (red curve). (For interpretation of the references to color in this figure legend, the reader is referred to the web version of this article.)

without mechanical strain applied [37–39]. One case of PVDF pipe failure in acid environment is also reported [40]. Despite the wide range of literature available on PVDF, no known data are reported for this specific copolymer [Kynarflex® 2800] subjected to the combined action of alkaline environment and mechanical strain. The only available information is the chemical resistance reported in the technical datasheet from the producer [11] and from the local distributor [10]. The degradation in alkaline environment [10% wt. NaOH, 80 °C] of similar materials [referred as "fluoroelastomers"] has been characterized by Mitra et al. [15]. Polymers belonging to the same class [PVDF-co-HFP] and from the same producer [Kynar Flex 2751 and UltraFlex RC-10] have been studied in potassium hydroxide [KOH] solution [32% wt. at room temperature] by Pagliaro and Lowy [16]. It was shown that these fluorocarbon co-polymers are susceptible to degradation in that particular alkaline environment similarly to PVDF homopolymer. It is therefore

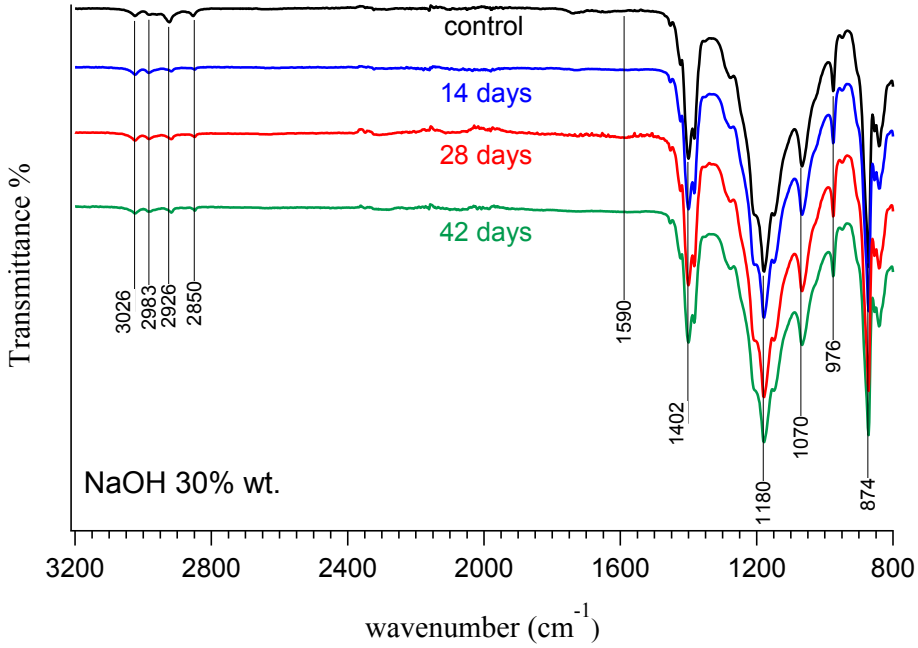


**Fig. 12.** FTIR spectra of artificially aged samples, after immersion in NaOH 30% wt. for different times.

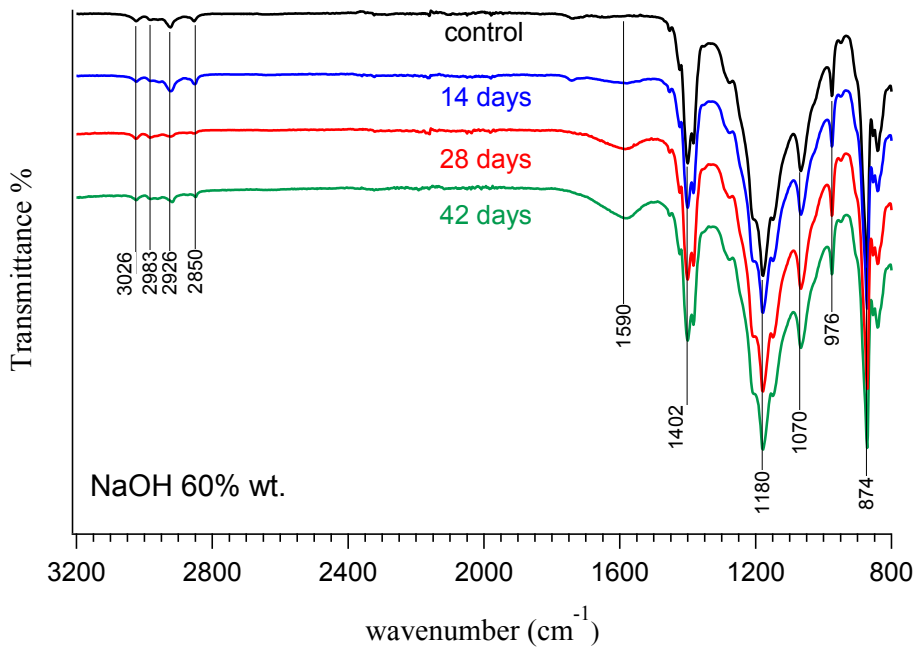


**Fig. 13.** FTIR spectra of artificially aged samples, after immersion in NaOH 60% wt. for different times.

plausible that Kynarflex® 2800 PVDF-co-HFP copolymer could show a similar response to concentrated NaOH (i.e. degradation and environmental stress cracking]. Moreover, Pagliaro and Lowy [16] attributed the reddish coloration to the formation of a —C═C—C═C—C— conjugated double bond system. This last hypothesis fits well with the reddish coloration [seen on cuts of failed pipes and on the surface of samples aged in 60% wt. NaOH] and the FT-IR peak seen on the same samples around 1590–1600 $cm^{-1}$ [attributable to the same conjugated double bond system]. It is worth pointing out that the Kynarflex® 2800 chemical resistance chart recommended a maximum concentration of NaOH $\leq$ 50% wt. at room temperature [20–25 °C], and NaOH $\leq$ 10% wt. [pH $\leq$ 13.5] if operating at 50 °C. The cleaning/disinfecting plant was running in a temperature range of 15–35 °C [therefore 10–15 °C above the standard room temperature], with a NaOH solution of 30% wt. Even if the chemical resistance chart has no data for this range, we can

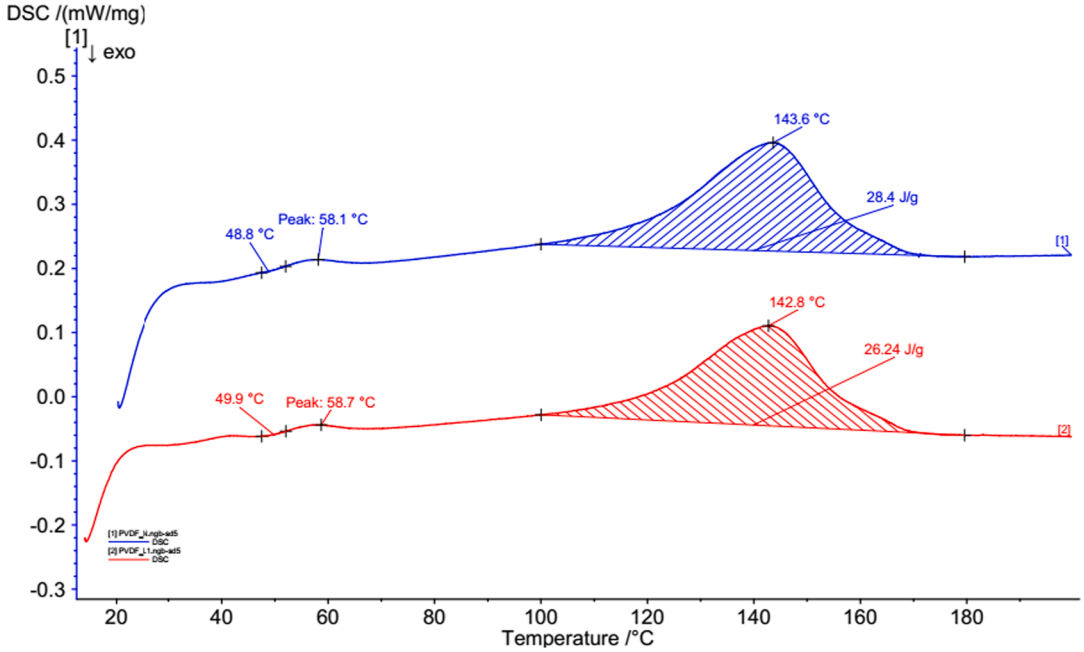


**Fig. 14.** DSC heating traces of samples obtained from new pipe (blue curve) and used pipe (red curve). (For interpretation of the references to color in this figure legend, the reader is referred to the web version of this article.)

speculate an intermediate maximum concentration [between 10% and 50% wt.]. Moreover, the reported bending radius of the pipes [between 90 and 130 mm], in its lower value, approaches closely the minimum bending radius recommended from the datasheet (85 mm].

## 5. Conclusions

### *5.1. Main findings*

The results of the background and technical documents show that the pipes in the cleaning/disinfection plant operated very close to the limits suggested by the technical datasheet and resistance chart. The analysis showed that the inner surface of the used tubes was subjected to a chemical degradation attributable to NaOH with visible dehydrofluorination. The mechanical strain of the pipe bendings, combined with this chemical degradation, led to a "solvent crazing", i.e. destruction of the surface integrity as a result of a chemical attack combined with mechanical stress. This conclusion was supported by SEM images that showed the presence of crazes on the surface, the formation and tearing of interconnecting material between crack edges and sodium fluoride deposits around damaged areas. According to simulated ageing experiment in alkaline environment, a 30% wt. NaOH solution alone is not enough to start a surface degradation phenomenon, while 60% wt. NaOH solution is able to degrade the polymer, but apparently without a deep dehydrofluorination. This is in line with info reported in the chemical resistance chart [11] and with previous works dealing with PVDF [9,12,14]. After these findings, probable causes of the failure are suggested:

(a) the concentration and/or the temperature of the solution was higher than those reported by the plant management [30% wt. NaOH, 10–35 °C]; it is possible that local high concentration areas [after water evaporation on drops] did form when the pipes were emptied or were not conveying the alkaline solution;
(b) the chemical resistance at 35 °C (not known from the datasheet) is actually lower than that expected at room temperature;
(c) the combined action of mechanical strain in the pipe bends (bending radius close to the minimum recommended one) and alkaline environment led to a localized failure.

### *5.2. Mitigation measures*

Some possible measures to avoid future failures in similar conditions are the following:

– reduce pipe bending radius to decrease the material strain;
– reduce operating temperature and/or NaOH concentration;
– wash properly the pipes with water after usage.

## Declaration of Competing Interest

The authors declare that they have no known competing financial interests or personal relationships that could have appeared to influence the work reported in this paper.

## References


[1] Q.M. Zhang, G. Kavarnos, Poly(Vinylidene Fluoride) (PVDF) and its Copolymers, in: Encyclopedia of Smart Materials [Internet]. Wiley Online Library, 2002. Available from: https://doi.org/10.1002/0471216275.
[2] F. Liu, N.A. Hashim, Y. Liu, M.R.M. Abed, K. Li, Progress in the production and modification of PVDF membranes, J. Membr. Sci. 375 (1) (2011) 1–27.
[3] G.J. Ross, J.F. Watts, M.P. Hill, P. Morrissey, Surface modification of poly(vinylidene fluoride) by alkaline treatment 1. The degradation mechanism, Polymer 41 (2000) 1685–1696.
[4] X. Cai, T. Lei, D. Sun, L. Lin, A critical analysis of the α, β and γ phases in poly(vinylidene fluoride) using FTIR, RSC Adv. 7 (25) (2017) 15382–15389.
[5] Y. Peng, P. Wu, A two dimensional infrared correlation spectroscopic study on the structure changes of PVDF during the melting process, Polymer 45 (15) (2004 Jul) 5295–5299.
[6] K.J. Kuhn, B. Hahn, V. Percec, M.W. Urban, Structural and quantitative analysis of surface modified poly(vinylidene fluoride) films using ATR FT-IR spectroscopy, Appl. Spectrosc. 41 (5) (1987) 843–847.
[7] M.-P. Gelin, B. Ameduri, Fluorinated block copolymers containing poly(vinylidene fluoride) or poly(vinylidene fluoride-cohexafluoropropylene) blocks from perfluoropolyethers: synthesis and thermal properties, J. Polym. Sci. Part A 41 (2002) 160–171.
[8] H. Kise, H. Ogata, Phase transfer catalysis in dehydrofluorination of poly(vinylidene fluoride) by aqueous sodium hydroxide solutions, J. Polym. Sci. Polym. Chem. Ed. 21 (12) (1983) 3443–3451.
[9] M.F. Rabuni, The contrastive study of chemical treatment on the properties of hydrophobic PVDF membrane, JASPE 2 (1) (2015) 30–43.
[10] Mebra Plaskik Italia SpA. KynarFlex 2800 Fluoropolimer datasheet [Internet]. Mebra Plaskik Italia SpA, 2021 (cited 2021 Mar 29). Available from: https://www.mebraplastik.com/images/pdf/fluoropolimero/1/TK.pdf.
[11] Arkema Inc., Kynar Polyvinylidene Fluoride Chemical Resistance Chart (Internet). Arkema Inc., 2007. Available from: https://www.extrememateriales-arkema.com/en/product-families/kynar-pvdf-family/chemical-resistance-fuel-resistance/download-kynar-pvdf-chemical-resistance-chart/.
[12] P. Hinksman, D.H. Isaac, P. Morrissey, Environmental stress cracking of poly(vinylidene fluoride) and welds in alkaline solutions, Polym. Degrad. Stab. 68 (2000) 299–305.
[13] P. Maccone, G. Brinati, V. Arcella, Environmental stress cracking of poly(vinylidene fluoride) in sodium hydroxide. Effect of chain regularity, Polym. Eng. Sci. 40 (3) (2000 Mar) 761–767.
[14] N. Awanis Hashim, Y. Liu, K. Li, Stability of PVDF hollow fibre membranes in sodium hydroxide aqueous solution, Chem. Eng. Sci. 66 (8) (2011) 1565–1575.
[15] S. Mitra, A. Ghanbari-Siahkali, P. Kingshott, K. Almdal, H. Kem Rehmeier, A.G. Christensen, Chemical degradation of fluoroelastomer in an alkaline environment, Polym. Degrad. Stab. 83 (2) (2004) 195–206.
[16] L.A. Pagliaro, D. Lowy, Interaction of polyvinylidene fluoride (PVDF)-based binders with strongly alkaline solutions, lgr. 29 (1) (2019) 17–31.
[17] R.P. Kambour, A review of crazing and fracture in thermoplastics, J. Polym. Sci. Macromol. Rev. 7 (1) (1973) 1–154.
[18] E.H. Andrews, L. Bevan, Mechanics and mechanism of environmental crazing in a polymeric glass, Polymer 13 (7) (1972 Jul) 337–346.
[19] E.J. Kramer, R.A. Bubeck, Growth kinetics of solvent crazes in glassy polymers, J. Polym. Sci. Polym. Phys. Ed. 16 (7) (1978) 1195–1217.
[20] G. Socrates, Infrared and Raman Characteristic Group Frequencies: Tables and Charts, third ed., 2004.
[21] Z. Yin, B. Tian, Q. Zhu, C. Duan, Characterization and application of PVDF and its copolymer films prepared by spin-coating and langmuir-blodgett method, Polymers 11 (12) (2019) 2033.
[22] V. Sencadas, S. Lanceros-Méndez, J.F. Mano, Characterization of poled and non-poled β-PVDF films using thermal analysis techniques, Thermochim Acta 424 (1–2) (2004) 201–207.
[23] R. Gregorio, D.S. Borges, Effect of crystallization rate on the formation of the polymorphs of solution cast poly(vinylidene fluoride), Polymer 49 (18) (2008) 4009–4016.
[24] J.J. Hermans, K. Keune, A. van Loon, P.D. Iedema, An infrared spectroscopic study of the nature of zinc carboxylates in oil paintings, J. Anal. At. Spectrom. 30 (7) (2015) 1600–1608.
[25] E.J. Henderson, K. Helwig, S. Read, S.M. Rosendahl, Infrared chemical mapping of degradation products in cross-sections from paintings and painted objects, Herit Sci. 7 (1) (2019 Dec) 71.
[26] J.E. Mark, Polymer Data Handbook, second ed., Oxford University Press, 1999.
[27] A.C. Gilby, J. Cassels, P.A. Wilks, Internal reflectance spectroscopy. III. Micro Sampling, Appl. Spectrosc. 24 (5) (1970) 539–543.
[28] K. Nakagawa, Y. Ishida, Annealing effects in poly(vinylidene fluoride) as revealed by specific volume measurements, differential scanning calorimetry, and electron microscopy, J. Polym. Sci. A-2 Polym. Phys. 11 (11) (1973) 2153–2171.
[29] M.F. Rabuni, N.M. Nik Sulaiman, M.K. Aroua, N.A. Hashim, Effects of alkaline environments at mild conditions on the stability of PVDF membrane: an experimental study, Ind. Eng. Chem. Res. 52 (45) (2013) 15874–15882.
[30] S. Bishop, D.H. Isaac, P. Hinksman, P. Morrissey, Environmental stress cracking of poly(vinyl chloride) in alkaline solutions, Polym. Degrad. Stab. 70 (3) (2000) 477–484.
[31] H. Shinohara, Fluorination of polyhydrofluoroethylenes. II. Formation of perfluoroalkyl carboxylic acids on the surface region of poly(vinylidene fluoride) film by oxyfluorination, fluorination, and hydrolysis, J Polym Sci Polym Chem Ed. 17 (5) (1979) 1543–1556.
[32] J.-L. Gacougnolle, S. Castagnet, M. Werth, Post-mortem analysis of failure in polyvinylidene fluoride pipes tested under constant pressure in the slow crack growth regime, Eng. Fail. Anal. 13 (1) (2006) 96–109.
[33] J. Marchand-Brynaert, N. Jongen, J.-L. Dewez, Surface hydroxylation of poly(vinylidene fluoride) (PVDF) film: 9.
[34] M. Wegener, W. Küunstler, R. Gerhard-Multhaupt, Poling behavior and optical absorption of partially dehydrofluorinated and uniaxially stretched polyvinylidene fluoride, Ferroelectrics 336 (1) (2006) 3–8.
[35] M. Alchikh, C. Fond, Y. FrEre, Discontinuous crack growth in poly (vinyl fluoride) by mechanochemical ageing in sodium hydroxide, Polym. Degrad. Stab. 5 (2010).
[36] M. Alchikh, C. Fond, Y. Frere, H. Pelletier, Mechanochemical degradation of poly(vinyl fluoride) by sodium hydroxide measured by microindentation, J. Mater. Sci. 6 (2010).
[37] F. Gao, J. Wang, H. Zhang, Y. Zhang, M.A. Hang, Effects of sodium hypochlorite on structural/surface characteristics, filtration performance and fouling behaviors of PVDF membranes, J. Membr. Sci. 519 (2016) 22–31.
[38] Q. Wang, H. Zeng, Z. Wu, J. Cao, Impact of sodium hypochlorite cleaning on the surface properties and performance of PVDF membranes, Appl. Surf. Sci. 428 (2018) 289–295.
[39] S.Z. Abdullah, P.R. Bérubé, Filtration and cleaning performances of PVDF membranes aged with exposure to sodium hypochlorite, Sep. Purif. Technol. 195 (2018) 253–259.
[40] Q. Guoquan, Y. Hongxia, Q. Dongtao, W. Bin, L. Houbu, Analysis of cracks in polyvinylidene fluoride lined reinforced thermoplastic pipe used in acidic gas fields, Eng. Fail. Anal. 99 (2019) 26–33.